

## Effects on the deformation-induced martensitic transformation in AISI 304 in external longitudinal turning

Berend Denkena<sup>a</sup>, Bernd Breidenstein<sup>a</sup>, Marc-André Dittrich<sup>a</sup>, Hai Nam Nguyen<sup>a,\*</sup>, Lara Vivian Fricke<sup>b</sup>, Hans Jürgen Maier<sup>b</sup>, David Zaremba<sup>b</sup>

<sup>a</sup> Institute of Production Engineering and Machine Tools, Leibniz University Hannover, An der Universität 2, 30823, Garbsen, Germany

<sup>b</sup> Institut für Werkstoffkunde (Materials Science), Leibniz University Hannover, An der Universität 2, 30823, Garbsen, Germany

### ARTICLE INFO

#### Keywords:

Tool geometry  
Deformation-induced martensitic transformation  
Flank face modification

### ABSTRACT

During the turning process of metastable austenitic steels, austenite is transformed into hard martensite by plastic deformation at low temperatures. This enables the production of components, which have both a hardened subsurface zone and a ductile core. Cryogenic cooling allows the subsurface zone to be hardened during machining, which leads to a shortening of the process chain. However, effects such as wear can make it challenging to adjust the properties of the subsurface zone during turning. By adjusting the tool microgeometry with a flank face modification, the wear condition can be kept constant for a certain period. In addition, the significance analysis with different tool microgeometries shows that only feed and initial temperature have a significant effect on the martensite formation.

### 1. Introduction

As a result of technical progress, demands regarding the performance of technical components are constantly increasing. Thus, many technical applications require components with a hardened subsurface zone while retaining a ductile core, such as camshafts or rotor shafts, guides, punches or bearing seats. The parallel increase in cost and time pressure creates a conflict of objectives within production. This conflict of objectives can be minimized through an innovative process chain.

So far, the hardening of the subsurface zone is usually achieved in processes with heat treatments. The chemical-thermal processes lead to a significant hardening of the subsurface zone. However, these processes are very time and energy intensive. Mechanical processes offer the advantage of a shorter process chain. However, the hardening effect is less pronounced (Brinksmeier et al., 2008b).

When machining metastable austenitic steels, the austenite is transformed into hard martensite during plastic deformation at low temperatures (Mayer et al., 2018). Cryogenic turning allows the subsurface zone to be hardened during machining, which leads to a considerable shortening of the process chain through the in-process increase of hardness during the turning process. In order to be able to precisely adjust the phase transformation in the process, it is beneficial to exclude as many disturbance variables as possible. One possibility for this is the

modification of the flank face. In this way, the wear condition remains constant for an extended time period.

The present paper examines the influence of the modification of the flank face on martensite formation for different process variables during turning. In addition, its influence is investigated compared to other tool microgeometries.

### 2. State of the art

The hardening effect of mechanical processes is usually the result of plastic deformation of the material layers close to the surface. Machining causes changes in the microstructure of the workpiece, such as grain elongation and refinement, formation of new (sub)grain boundaries, and an increase in dislocation density below the workpiece surface (Jawahir et al., 2011). Dislocations describe linear structural defects of a crystal lattice and, with increasing number per volume unit, increasingly impede each other in their movement. This results in strain hardening, which increases the resistance to plastic deformation. Outeiro et al. show that this increases microhardness upon machining (Outeiro et al., 2015).

The hardening effect in mechanical processes is correlated to the contribution of compressive residual stresses in the subsurface zone of the workpiece (Meyer, 2012). Due to the unique properties of metastable austenitic steel, in addition to strain hardening and the contribution of

\* Corresponding author.

E-mail address: [nguyen@ifw.uni-hannover.de](mailto:nguyen@ifw.uni-hannover.de) (H.N. Nguyen).

compressive residual stresses, an increase in hardening in the subsurface zone can be achieved by a phase transformation from austenite to martensite. As a result of the martensite formation, tensile strength and hardness increase. Martensite generally has higher strength and is harder than austenite, because the distorted crystal structure has higher resistance to the motion of dislocations (Totten, 2006). Pranke et al. show that microhardness increases linearly with increasing martensite content (Pranke et al., 2015).

### 2.1. The martensite phase transformation

The phase transformation in metastable austenitic steel is based on different stability of austenite and martensite and the endeavour of each system to reach the energetically most favourable state. One criterion for the transformation tendency into the more stable state is the chemical driving force  $\Delta G_{\text{chem}}$  (Gibbs free energy), which results from the energy difference between the two phases. This difference increases with decreasing temperature and reaches  $\Delta G_{\text{min}}$  at the  $M_s$ -temperature.  $\Delta G_{\text{min}}$  is the minimum energy required to trigger a transformation of the metastable austenite into the more stable martensite phase (Tamura, 1982). At the  $M_s$ -temperature, the purely thermally-induced phase transformation can set in.

Under the additional influence of mechanical stress, however, the phase transformation from austenite to martensite can be induced above the  $M_s$ -temperature (Patel and Cohen, 1953). A prerequisite for this is that the mechanically-induced free energy  $\Delta G_{\text{mech}}$  due to the applied stress is so large that, together with the chemical driving force  $\Delta G_{\text{chem}}$ , the minimum required energy  $\Delta G_{\text{min}}$  for transformation is achieved (Tamura, 1982). The highest temperature up to which this type of martensitic transformation can still occur is called the  $M_d$ -temperature (Angel, 1954; Weiß et al., 2016).

### 2.2. Influence of the turning process on the deformation-induced martensitic transformation

In order to avoid additional thermal hardening and thus shorten the process chain, the combination of hardening and machining with the same machine tool is an option (Brinksmeier et al., 2008a). In metastable austenitic steels, hardening of the subsurface zone can be achieved by deformation-induced martensitic transformation as a result of low temperatures and deformation (Llewellyn, 1997).

Using carbon dioxide snow cooling, Aurich et al. showed that cryogenic cooling can be used to achieve hardening of metastable austenitic steels already during the turning process (Aurich et al., 2014). The influence of the cutting parameters with this cooling system is investigated in (Mayer et al., 2018). It is shown that a high feed rate, a low cutting speed and a low depth of cut cause the highest martensitic transformation. Considering the impact of the tool properties, the higher the cutting edge radii and chamfer angles, the higher the martensitic transformation (Hotz and Kirsch, 2020). However, to set different martensite levels, disturbances resulting from increasing tool wear can affect the martensitic transformation.

### 3. Experimental approach to investigate the martensitic transformation

To adjust the phase transformation from austenite to martensite in the turning process, the exclusion of disturbance variables in the form of tool wear is beneficial. This can be realized by modifying the cutting tool. Denkena et al. modified the tool flank face by using an undercut of the flank face during hard turning (Denkena et al., 2008). This limits the wear process on the flank face geometrically. Due to the temporary continuity of the wear condition, the contact conditions do not change significantly during machining. Therefore, under otherwise identical machining conditions, both the thermal-mechanical loads on the subsurface zone and the resulting component properties remain almost

constant.

The aim of the present study is to use this advantage and to analyze the effect of this modification of tool microgeometry on the phase transformation within the turning process. For this purpose, the influence of the flank face modification is investigated with varying process parameters. The results are compared with other tool microgeometries such as untreated conventional tool geometries and those with rounded cutting edges. In the first step, the effects of different process variables and different starting temperatures are investigated. Based on that, a defined range of the process parameters for further investigation is determined and the effects of different tool microgeometries are taken into consideration.

With the removal of a part of the flank face along the cutting edge, the effective contact length of the tool with the workpiece and, consequently, the amount of flank wear occurring during the machining process is geometrically limited to a defined web width  $S_b$  (Fig. 1). This leads to a wear reserve that delays the increase in wear for a given cutting time and thus extends tool life. The duration of the wear delay depends on the volume of the wear reserve and is determined by the depth of the resulting web  $S_t$ . The smaller  $S_b$ , the faster the configured wear delay is used up. However, with higher  $S_b$ , the cutting edge is less stable and can break off. After several stability experiments, the following setup of  $S_b = 280 \mu\text{m}$  and  $S_t = 50 \mu\text{m}$  is chosen, which guarantees a stable process.

### 4. Experimental investigations on the martensitic transformation

The experimental investigations include the generation of the flank face modification as well as the cutting edge rounding by laser ablation on uncoated carbide indexable inserts (CNMA120408 by Kennametal). A DMG-Lasertec 40, equipped with a Q-Switch-Nd:YVO<sub>4</sub> laser, is used for this purpose. The generation of the flank face modification with the modified contact area takes place in two process steps. In the first process step, the contact area is lasered on the web of the flank face, whereby only a very small amount of material is removed. The purpose of this process step is to expose the grain-shaped cutting material particles directly in the area below the cutting edge so that a rough surface is created, representing wear. Finally, in the following process step, the undercut of the flank face is machined using the same program sequence with adapted laser parameters. The width and depth measurements of the created web by the flank face modification are performed with the help of a Keyence VHX-600DSO digital microscope. The GFM MikroCAD, which works with digital fringe projection, is used to evaluate shape and size of the created cutting edge roundings. A cutting edge rounding with a target value of  $\bar{r} = 80 \mu\text{m}$  (mean value is  $85 \mu\text{m}$  with a standard

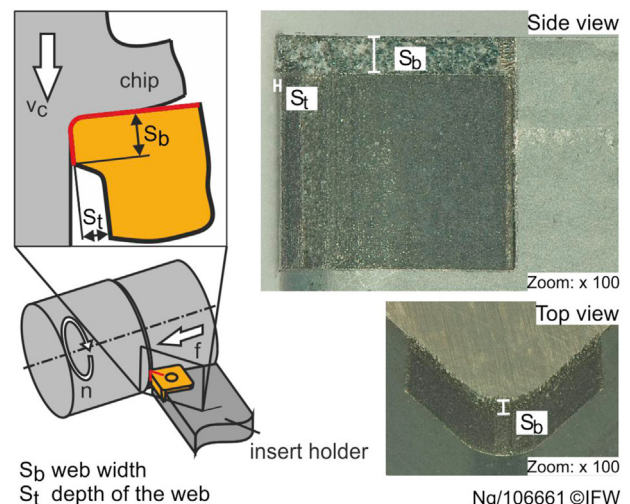


Fig. 1. Flank face modification.

deviation of 9  $\mu\text{m}$ ) is used. In contrast, the unmodified indexable insert has an average cutting edge rounding of  $\bar{S} = 3 \mu\text{m}$  with a standard deviation of 0.2  $\mu\text{m}$ . The prepared inserts are clamped on a tool holder (MCN12L 2525M12) which results in a rake angle of  $\gamma = -6^\circ$ , a tool cutting edge inclination of  $\lambda = -6^\circ$  and a tool cutting edge angle of  $\kappa = 95^\circ$ .

The turning experiments are carried out on a universal turning center CTX 800 4A from DMG MORI. No in-process cooling or lubricant is used. In order to measure force, the tool holder is placed in a 3-component dynamometer type 9129A from Kistler. The measuring principle is based on the piezoelectric effect. The tool orthogonal rake angle  $\gamma$  and tool cutting edge inclination  $\lambda$  are  $-6^\circ$  each. The metastable austenitic CrNi steel AISI 304 (1.4301) is used as test material. This is a corrosion-resistant steel that is widely used in industry (Totten, 2006). The material is solution annealed at 1050  $^\circ\text{C}$  for 45 min and slowly cooled in an argon atmosphere to obtain a homogeneous microstructure. The workpieces have a diameter of 49.7 mm and a length of 50 mm.

The following measuring systems are used to determine the relevant target values. The qualitative evaluation of the martensite content is completed by determining the ferromagnetic content with a Feritscope MP30 from Fischer, which is based on a magnetic-inductive measurement. Ferromagnetic structure components (in this case  $\alpha'$ -martensite) in the subsurface zone change the magnetic permeability, which is detected by the Feritscope (Talonon et al., 2004). However, the absolute value of the martensite content cannot be detected with a Feritscope, because a calibration with samples made of the same steel and containing specific amounts of martensite would be necessary. Furthermore, the penetration depth of the measurement depends on the ferromagnetic properties of the microstructure. A higher ratio of martensite results in a lower penetration depth. This can have an effect on the measurement values. Within this kind of steel, only  $\alpha'$ -martensite created by deformation results in an increase in ferromagnetic phase content. Therefore, this conventional measuring instrument is sufficient to determine and compare the relative proportion of martensite content due to the variation of the process parameters. The determined values are normalized values as detailed below.

Using X-ray diffraction (XRD), austenitic and martensitic phases can be distinguished from each other. XRD investigations are used to determine the retained austenite contents. The X-ray diffractometer used is a Seifert XRD 3003 TT from General Electric. For steel materials, Cr-K $\alpha$  radiation is generally used because it is very surface sensitive and does not excite the iron to fluoresce, which would interfere with the measurements. To determine the martensite content over the entire depth of the sample, 10–30  $\mu\text{m}$  are removed by etching before a new measurement is taken. This is repeated until no more martensite is detected. The determined martensite contents are integrated across the different depths and divided by the total volume to determine the total average volume content of martensite within the subsurface zone. Integration is performed for all samples up to a depth of 243  $\mu\text{m}$ , which is the maximum transformation depth in the tests where martensite was still detected. Due to the laborious process, not all samples could be analyzed with XRD, so it is only used for extreme values of the Feritscope results to verify the trends observed.

The automatic Vickers-hardness testing system Qness Q10 A+ is used to record the microhardness according to Vickers HV0.1 at a depth of 50  $\mu\text{m}$ .

#### 4.1. Influence of different process parameters

In order to investigate the different influencing factors on martensitic transformation during turning, different parameters are varied in the first series of experiments. The examined range and levels of the different process parameters can be seen in Table 1. One single parameter is varied at a time, while the remaining parameters are each held at a previously defined reference state. The following combination of parameters is

**Table 1**  
Process parameters.

Cutting speed [m/min]	Feed [mm]	Depth of cut [mm]	Initial workpiece temperature [ $^\circ\text{C}$ ]
30	0.2	0.2	20
50	0.6	0.35	0
70	0.8	0.5	-10
90	1.0	1.0	-20
110		1.5	-30
130			-40
150			-70
			-115
			-150
			-193

defined as reference state: Feed  $f = 0.2 \text{ mm}$ , depth of cut  $a_p = 0.2 \text{ mm}$ , cutting speed  $v_c = 150 \text{ m/min}$ , and an initial workpiece temperature  $T = -115 \text{ }^\circ\text{C}$ . The workpieces are placed in a container filled with liquid nitrogen before the actual turning process. The different initial temperatures of the workpieces are adjusted over various periods of time in the nitrogen. For example, the workpiece has to be in the liquid nitrogen for 3 min and 30 s to reach a temperature of  $-70 \text{ }^\circ\text{C}$  in the core. The temperature is measured with a type K thermocouple in a borehole in the core of the workpieces directly before they are placed into the turning center. In the region of a target temperature of  $-70 \text{ }^\circ\text{C}$  for example, the workpiece warms up with approximately 1.5  $^\circ\text{C}$  per minute after leaving the liquid nitrogen. For the experiments, the workpiece is cooled below the target temperature and is placed in the machine tool if the difference between the actual and target temperature is 1  $^\circ\text{C}$  (thus at  $-71 \text{ }^\circ\text{C}$  in the example here). This gives enough time to clamp the workpiece and start the turning process. At  $-70 \text{ }^\circ\text{C}$  in the core before machining, the temperatures on the surface of the workpiece show a mean value of  $-39 \text{ }^\circ\text{C}$  with a standard deviation of 3  $^\circ\text{C}$ . The temperature values are taken from the borehole, because it is more practicable to measure the temperature there under the same conditions. The temperatures in the borehole immediately after machining have a mean value of  $-59 \text{ }^\circ\text{C}$  with a standard deviation of 4  $^\circ\text{C}$ , depending on the different chosen process parameters and consequently the duration of the process. The diameters are measured directly after machining at the beginning and at the end of the workpiece. They do not show any significant difference between each other or to the target diameter. Therefore, a variation of the depth of cut during the process is not expected. If the diameter of the machined workpiece is measured when it reaches room temperature again, a maximum deviation of 0.1 mm from the target diameter can be observed. The workpiece expanded at room temperature. Hence, the measurements after warming up thus show in contrast a lower depth of cut. Nevertheless, the depth of cut directly after the process is considered for the experiments, because this is the actual depth of cut in the process.

The effects of the parameters based on the Feritscope investigations show that temperature has the greatest influence on martensitic transformation (Fig. 2). The lower the initial temperature of the workpiece, the more martensite is formed.

The chemical driving force  $\Delta G_{\text{chem}}$  increases with decreasing temperature, which promotes the transformation to martensite during deformation. In addition, decreasing temperatures lead to a reduced stacking fault energy, which also leads to an increased martensite formation (Olson and Cohen, 1975). The stacking fault energy describes the energy required to generate a planar lattice defect. As a result, the deformation-induced  $\epsilon$ -martensite formation and the deformation-induced  $\gamma \rightarrow \alpha'$  or  $\gamma \rightarrow \epsilon \rightarrow \alpha'$ -martensitic transformation are likely to occur during deformation.

On the basis of the chemical composition of the material alone and by excluding other factors, the temperatures  $M_{d30}$  and  $M_s$  can be approximated with the formulas from (Angel, 1954; Eichelmann, Jr., G.H. and Hull, 1952).  $M_{d30}$  is the temperature at which 50% martensite is formed as a result of 30% plastic deformation. It is used instead of  $M_d$  for the

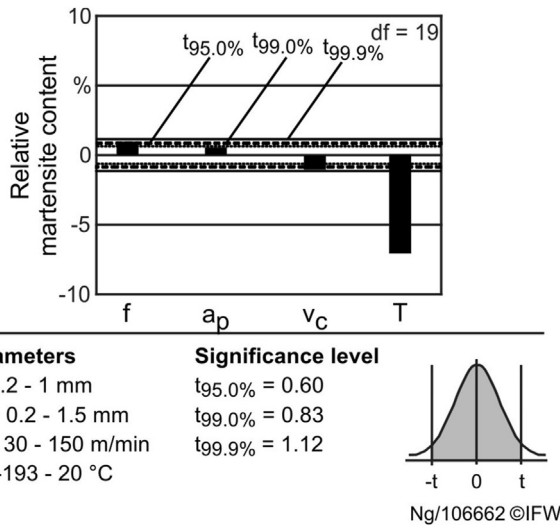


Fig. 2. Effects of the process parameters on martensite formation.

purpose of simplified determinability. In the present case,  $M_{d30} \approx 0 \text{ }^\circ\text{C}$  is the calculated result (Fricke et al., 2021a). The actual  $M_d$  temperature is higher, theoretically allowing machining without prior cooling of the components. However, the experiments show that the turning process at room temperature does not lead to a significant phase transformation. With a calculated  $M_s \approx -273 \text{ }^\circ\text{C}$ , it follows that a transformation without any superimposed mechanical stress is not possible. During the experiments, this has also been confirmed with the lowest selected temperature of  $T = -193 \text{ }^\circ\text{C}$ .

4.2. Influence of the process parameters with different tool microgeometries

After showing in 4.1 that temperature has a great influence on phase transformation, the influence of the process parameters is examined in detail in the following. These parameters can easily be adjusted during the turning process, and thus serve primarily as control variables to set desired subsurface zone properties in the workpiece. For this purpose, an additional significance analysis is performed to investigate the influence of each process variable. Based on the previous experiments, the range of cutting speed is adjusted in a lower value range. This reduces the

temperature in the process, which is beneficial for the martensitic transformation. The variation of the process parameters was carried out with different tool microgeometries. Thus, it can be investigated whether the process variables have different influences on the martensitic transformation based on the tool microgeometry. The process variables feed  $f$ , depth of cut  $a_p$  and cutting speed  $v_c$  are each varied in two factor levels:  $f$  is varied at 0.3 mm and 0.7 mm,  $a_p$  at 0.2 mm and 0.5 mm and  $v_c$  at 30 m/min and 70 m/min. The experiments are performed in a full factorial manner. The samples are immersed in liquid nitrogen before processing and the experiments are started when a core temperature of  $T = -70 \text{ }^\circ\text{C}$  is reached. Detailed data of the experiments is presented in the Appendix (Table 3).

The results of the significance analyses show that only the feed  $f$  is significant for the martensitic transformation both for the unmodified indexable insert (Fig. 3, a) and for the one with flank face modification (Fig. 3, b). The same result can be observed for the rounded indexable inserts.

The mechanical load increases with increasing feed. This is due to the fact that the feed influences the cross-section of the undeformed chip, and thus directly affects the resistance against penetration of the cutting edge. In contrast to the investigations of Mayer et al., (2018), the depth of cut and the cutting speed are not relevant. A reduction of the phase transformation due to higher temperatures because of higher friction with increasing cutting speed is not observed here. A possible explanation is that, in contrast to Mayer et al. the workpieces were completely cooled during these experiments. Therefore, the effect is not significant with the small step distance of this parameter. Due to the complete cooling, it can also be observed that an increasing depth of cut does not lead to a reduction in martensitic transformation. However, an increase in martensite content due to higher forces as a result of the higher depth of cut is also not significant. This indicates that most of the mechanical stress is applied to the chip and not to the workpiece surface.

The influence of tool wear is taken into account in the screening experiments via block formation. An indexable insert is used up to a maximum of four times. The mean value of the flank wear after fourfold use is  $60 \text{ }\mu\text{m}$  with a standard deviation of  $9 \text{ }\mu\text{m}$ . It is assigned to the appropriate blocks depending on the frequency of use. The effect of the blocks thus represents the influence of wear on the martensitic transformation. It can be seen in Fig. 3 that the effect of wear is reduced by using the flank face modification compared to the unmodified insert.

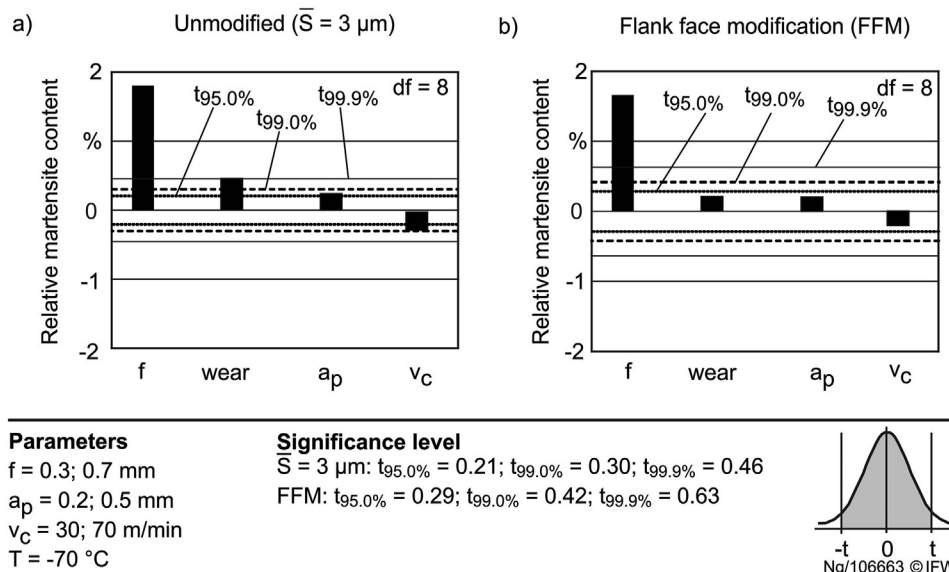


Fig. 3. Effects of the process parameters with flank face modification (b) compared to the unmodified indexable insert (a).

4.3. Influence of flank face modification compared to cutting edge rounding

The results of the flank face modification are combined with data from the unmodified indexable insert to determine the effect of altering tool microgeometry. Likewise, the results of the cutting edge rounding are compared to the unmodified one. With this pairwise comparison, the difference of the martensitic transformation caused by the tool microgeometries can be identified. The influence of the flank face modification compared to the unmodified insert is not significant (Fig. 4, a)). In contrast, the cutting edge rounding has a significant influence on the formation of martensite (Fig. 4, b)).

Considering the measured forces, it can be seen that the flank face modification has especially a significant effect on the passive force (Fig. 5). This is due to the fact that the passive force increases with higher flank wear (Denkena et al., 2008). The increased passive force due to the flank face modification results in compressive stresses. For the formation of martensite, shear stresses are more of an advantage than compressive stress because the martensite elemental cell has a higher volume than the austenite one. Thus, normal stresses can have both a supporting and an inhibiting effect depending on the direction of the mechanical stresses as well as the simultaneous changes in shape during martensite formation (Patel and Cohen, 1953). Since the phase transformation from austenite to martensite increases the volume, tensile and shear stresses are more advantageous for martensite formation (Totten, 2006). Nonetheless, the effect of the flank face modification on the passive force is also smaller compared to the effect caused by the feed (Fig. 5). Thus, the amount of passive force increase may be essential, because the feed has a significant effect on the phase transformation. From this, it can be concluded that the increase of the passive force with the flank face modification may not be sufficient for significantly increasing the martensitic transformation. In addition, the effect of the flank face modification on the passive force is smaller than the effect caused by the cutting edge roundings (Figs. 5 and 6).

In contrast, the rounded indexable inserts have significantly increased all force components (Fig. 6), which generally increases the mechanical load. Of the existing martensitic shearing systems, certain ones are preferably activated during the mechanically-induced martensitic transformation. This is the case for those on which the greatest amount of mechanical work is performed due to the favourable orientation to the direction of stress (Fricke et al., 2021b). Higher stresses are required in order to activate shear systems that are less favourable to the direction of

stress and to continue the martensite formation. Another possibility is to change the direction of stress by changing the tool cutting edge angle in a second machining process, for example. With an increase of the mechanical load in all spatial directions due to the rounding of the cutting edge, the martensite formation increases in general. This was also confirmed in tensile tests in (Murr et al., 1982) in which a higher martensite content was found under biaxial load as compared to uniaxial tensile load.

The XRD measurement results confirm the observations obtained with the Feritscope (Table 2). The samples pertaining to the maximal and minimal values from the Feritscope investigations are analyzed with XRD regarding all three different tool microgeometries. The highest transformation is achieved with the cutting edge roundings with a high feed rate at 13.1% martensite content. The lowest transformation can be observed with the unmodified tools with low feed with 5.6% martensite content. The XRD evaluation results show large scattering. This is due to the fact that the samples show textures due to the turning process. The measurement and evaluation methods, however, are based on the assumption that the samples are without texture.

The average microhardness of unmachined samples is 172 HV0.1. A similar result can be seen in the microhardness development, which confirms the contribution of martensitic transformation to microhardness increase. The maximum microhardness is achieved with cutting edge rounding and high feed rate at around 375 HV0.1. Lower microhardness values can be observed in the unmodified tools with low feed at around 290 HV0.1. Microhardness values of a similar magnitude are also found in Ref. (Hotz and Kirsch, 2020). The average thickness of the hardened layer obtained after machining with cutting edge rounding and high feed rate is 478 μm with a maximum of 580 μm and a minimum of 400 μm.

5. Conclusion and outlook

Deformation-induced martensite formation during the machining can be utilized to produce components with a hard subsurface zone and a ductile core. The existing process chain can be shortened by accomplishing hardening during the turning process in an adjustable manner. Thus, the influence of various parameters such as feed, depth of cut, cutting speed and initial workpiece temperature on the phase transformation is investigated. This is done with different tool microgeometries like cutting edge roundings and flank face modification.

In the experimental studies, it was found that the temperature appears

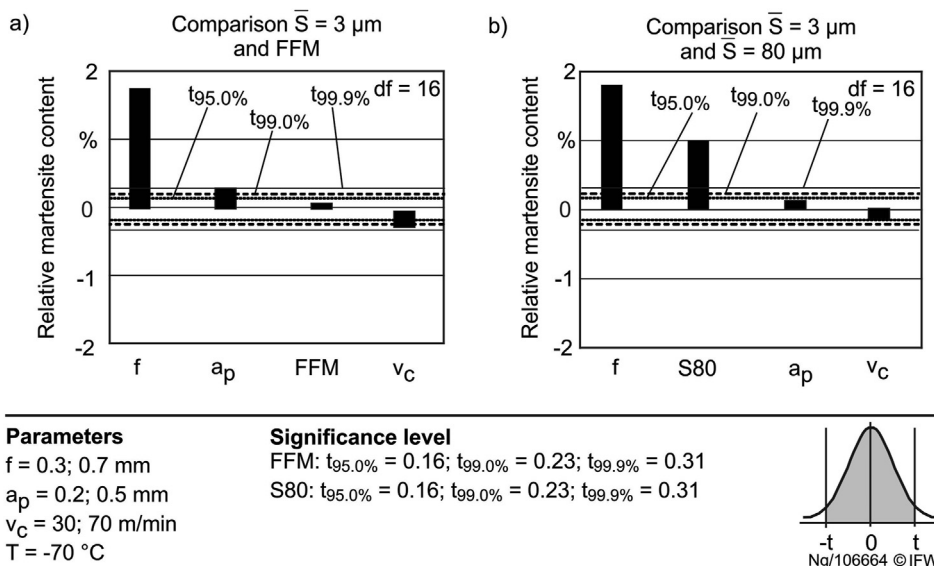


Fig. 4. Effects of flank face modification (FFM) (a) and of cutting edge rounding (S80) (b).

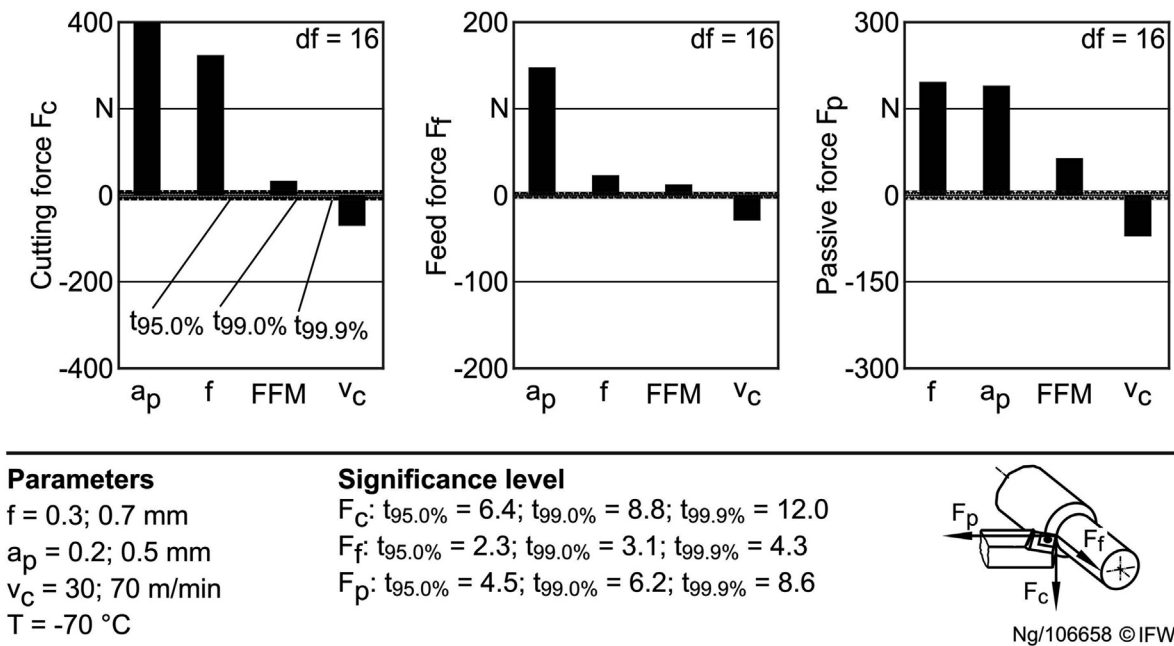


Fig. 5. Effects of the flank face modification (FFM) on process forces.

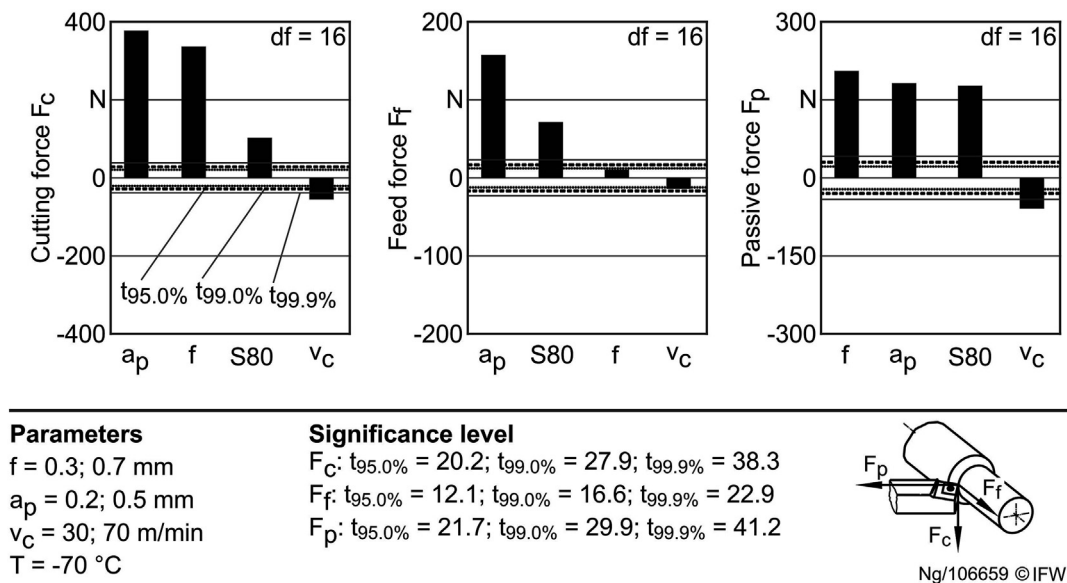


Fig. 6. Effects of the cutting edge rounding (S80) on the process forces.

**Table 2**  
 Comparison of the different measurements for different tool microgeometries and process parameters (mean value (standard deviation)).

Tool microgeometry	Feritscope [%]	XRD [%]	Microhardness [HV0.1]
<b>Unmodified</b>			
Maximum	3.7 (0.2)	11.1 (4.5)	352 (30)
Minimum	1.9 (0.3)	5.6 (2.9)	290 (24)
<b>Flank face modification</b>			
Maximum	3.6 (0.2)	11.9 (3.7)	358 (27)
Minimum	1.9 (0.2)	9.3 (2.1)	325 (29)
<b>Rounded cutting edge</b>			
Maximum	4.6 (0.2)	13.1 (3.2)	385 (21)
Minimum	2.4 (0.1)	9.2 (3.5)	360 (28)

to have the greatest influence on the phase transformation. The

temperature influences the chemical driving force and the stacking fault energy. As temperature decreases, the chemical driving force increases, resulting in more martensite being formed. Further, the stacking fault energy decreases, favoring lattice defects and displacements, which is conducive to martensitic transformation. In terms of process parameters, only the feed is significant. As the feed increases, martensitic transformation also increases due to the higher mechanical stress.

The rounding of the indexable insert causes higher mechanical stresses and consequently more martensite can be obtained than with an unmodified indexable insert. A flank face modification, which is introduced here for the formation of deformation-induced martensite, on the other hand, causes a phase transformation similar to that one of the unmodified indexable insert. Due to the limitation of the flank face which results in the limitation of tool wear, the wear condition remains constant for a certain period. This reduces the influence of wear on the phase

transformation, which is beneficial for the creation of a desired and predetermined martensite content by machining. The potential effects of wear on the deformation-induced martensite formation were analyzed which is the main novelty of the contribution.

Alternatives to the current pre-cooling of the workpiece can be the use of pre-cooling and cooling during the process by using CO<sub>2</sub> in the machine tool itself. The integration of a CO<sub>2</sub> cooling system and the investigation thereof are the subjects of current work. Due to the significance of the feed and temperature, these parameters will be further investigated in future work as control variables and used for setting desired subsurface zone properties.

## Appendix

**Table 3**

Feritscope values and forces for different tool microgeometries and process parameters of the screening experiments.

Tool microgeometry	f [mm]	a <sub>p</sub> [mm]	v <sub>c</sub> [m/min]	F <sub>c</sub> [N]	F <sub>f</sub> [N]	F <sub>p</sub> [N]	Feritscope [%]
<b>Unmodified</b>							
	0.3	0.2	30	199.8	52.4	161.6	1.8
	0.7	0.2	70	374.2	57.2	236.8	2.9
	0.7	0.5	30	983.3	232.9	582.4	4.1
	0.3	0.5	30	529.0	222.3	335.6	2.1
	0.3	0.2	70	221.7	59.3	141.2	1.6
	0.7	0.2	30	457.2	81.4	339.3	3.4
	0.3	0.5	70	450.3	161.1	247.0	1.5
	0.7	0.5	70	857.6	195.0	446.3	3.7
	0.3	0.5	30	531.1	223.2	334.5	1.7
	0.3	0.2	30	203.5	53.6	163.8	1.6
	0.7	0.2	30	457.3	81.0	337.2	3.3
	0.3	0.2	70	225.8	60.1	144.5	2.0
	0.7	0.2	70	373.0	56.7	236.7	3.2
	0.3	0.5	70	448.3	169.9	263.8	1.6
	0.7	0.5	30	1010.0	244.3	596.0	4.4
	0.7	0.5	70	869.2	195.4	443.5	3.7
<b>Flank face modification</b>							
	0.7	0.5	30	1018.6	256.3	646.9	4.4
	0.3	0.5	30	538.0	228.2	376.5	2.1
	0.7	0.2	30	461.6	80.7	359.4	3.7
	0.3	0.2	70	241.3	65.9	190.7	2.3
	0.3	0.2	30	260.8	68.4	225.4	1.5
	0.3	0.5	70	475.7	170.3	284.4	1.7
	0.7	0.2	70	378.8	66.1	336.3	2.9
	0.7	0.5	70	923.6	227.4	585.3	3.5
	0.7	0.5	70	935.1	229.9	584.0	3.8
	0.3	0.2	30	258.9	68.1	217.7	2.0
	0.3	0.5	70	478.0	172.1	286.1	1.6
	0.7	0.2	30	488.2	81.3	382.5	3.3
	0.3	0.5	30	543.7	229.7	376.2	1.8
	0.7	0.2	70	389.0	66.7	336.9	3.2
	0.3	0.2	70	244.7	65.9	187.7	2.0
	0.7	0.5	30	1039.1	264.6	654.6	4.0
<b>Rounded cutting edge</b>							
	0.7	0.5	70	993.2	311.2	663.4	4.3
	0.3	0.2	30	363.9	159.5	356.6	3.1
	0.3	0.5	70	520.5	257.9	390.5	2.4
	0.7	0.2	30	545.4	99.8	499.0	4.2
	0.3	0.5	30	597.3	290.7	429.9	2.2
	0.7	0.2	70	498.9	96.5	425.3	4.4
	0.3	0.2	70	270.0	95.6	254.1	2.8
	0.7	0.5	30	1020.3	275.4	743.1	4.9
	0.7	0.5	30	1046.7	301.0	755.5	4.7
	0.7	0.2	70	605.5	138.1	494.2	4.6
	0.3	0.2	30	324.3	116.2	313.5	2.9
	0.3	0.5	70	520.2	271.3	427.7	2.5
	0.3	0.5	30	576.2	279.8	445.6	2.6
	0.7	0.2	30	540.1	104.3	503.0	4.6
	0.7	0.5	70	996.6	330.8	742.2	4.8
	0.3	0.2	70	361.2	151.6	362.7	3.2

## References

- Angel, T., 1954. Formation of martensite in austenitic stainless steels. In: Iron Steel Inst. J. (Ed.), 177, pp. 165–174. Available online at: <https://ci.nii.ac.jp/naid/10026799705/en/>.
- Aurich, Jan C., Mayer, Patrick, Kirsch, Benjamin, Eifler, Dietmar, Smaga, Marek, Skorupski, Robert, 2014. Characterization of deformation induced surface hardening during cryogenic turning of AISI 347. *CIRP Annals* 63 (1), 65–68. <https://doi.org/10.1016/j.cirp.2014.03.079>.
- Brinksmeier, E., Garbrecht, M., Meyer, D., 2008a. Cold surface hardening. *CIRP Annals* 57 (1), 541–544. <https://doi.org/10.1016/j.cirp.2008.03.100>.
- Brinksmeier, E., Garbrecht, M., Meyer, D., Dong, J., 2008b. Surface hardening by strain induced martensitic transformation. *Prod. Eng. Res. Dev.* 2 (2), 109–116. <https://doi.org/10.1007/s11740-007-0060-6>.
- Denkena, Berend, Boehnke, David, Meyer, Roland, 2008. Reduction of wear induced surface zone effects during hard turning by means of new tool geometries. *Prod. Eng. Res. Dev.* 2 (2), 123–132. <https://doi.org/10.1007/s11740-008-0089-1>.
- Eichelmann Jr., G.H., Hull, F.C. (Eds.), 1952. Effect of Composition on Temperature of Spontaneous Transformation of Austenite to Martensite in 18-8-type Stainless Steel. American Society for Metals – Meeting: American Society for Metals. Available online at: [https://www.tib.eu/de/suchen/id/ei-backfile%3Ac84\\_13d77b9fa7d318f8dM314819817173212](https://www.tib.eu/de/suchen/id/ei-backfile%3Ac84_13d77b9fa7d318f8dM314819817173212).
- Fricke, Lara V., Nguyen, Hai Nam, Breidenstein, Bernd, Zaremba, David, Maier, Hans Jürgen, 2021a. Eddy current detection of the martensitic transformation in AISI304 induced upon cryogenic cutting. *In steel research int* 92 (1), 2000299. <https://doi.org/10.1002/srin.202000299>.
- Fricke, Lara Vivian, Gerstein, Gregory, Breidenstein, Bernd, Nguyen, Hai Nam, Dittrich, Marc-André, Maier, Hans Jürgen, Zaremba, David, 2021b. Deformation-induced martensitic transformation in AISI304 by cryogenic machining. *Mater. Lett.* 285, 129090. <https://doi.org/10.1016/j.matlet.2020.129090>.
- Hotz, Hendrik, Kirsch, Benjamin, 2020. Influence of tool properties on thermomechanical load and surface morphology when cryogenically turning metastable austenitic steel AISI 347. *J. Manuf. Process.* 52, 120–131. <https://doi.org/10.1016/j.jmapro.2020.01.043>.
- Jawahir, I.S., Brinksmeier, E., M'Saoubi, R., Aspinwall, D.K., Outeiro, J.C., Meyer, D., et al., 2011. Surface integrity in material removal processes: Recent advances. *CIRP Annals* 60 (2), 603–626. <https://doi.org/10.1016/j.cirp.2011.05.002>.
- Llewellyn, D.T., 1997. Work hardening effects in austenitic stainless steels. *Mater. Sci. Technol.* 13 (5), 389–400. <https://doi.org/10.1179/mst.1997.13.5.389>.
- Mayer, Patrick, Kirsch, Benjamin, Müller, Christopher, Hotz, Hendrik, Müller, Ralf, Becker, Steven, et al., 2018. Deformation induced hardening when cryogenic turning. In *CIRP Journal of Manufacturing Science and Technology* 23, 6–19. <https://doi.org/10.1016/j.cirpj.2018.10.003>.
- Meyer, Daniel, 2012. Cryogenic deep rolling – an energy based approach for enhanced cold surface hardening. *CIRP Annals* 61 (1), 543–546. <https://doi.org/10.1016/j.cirp.2012.03.102>.
- Murr, L.E., Staudhammer, K.P., Hecker, S.S., 1982. Effects of strain state and strain rate on deformation-induced transformation in 304 stainless steel: Part II. Microstructural study. In *MTA* 13 (4), 627–635. <https://doi.org/10.1007/BF02644428>.
- Olson, G.B., Cohen, Morris, 1975. Kinetics of strain-induced martensitic nucleation. In *MTA* 6 (4), 791–795. <https://doi.org/10.1007/BF02672301>.
- Outeiro, J.C., Campocasso, S., Denguir, L.A., Fromentin, G., Vignal, V., Poulachon, G., 2015. Experimental and numerical assessment of subsurface plastic deformation induced by OFHC copper machining. In *CIRP Annals* 64 (1), 53–56. <https://doi.org/10.1016/j.cirp.2015.04.080>.
- Patel, J.R., Cohen, M., 1953. Criterion for the action of applied stress in the martensitic transformation. *Acta Metall.* 1 (5), 531–538. [https://doi.org/10.1016/0001-6160\(53\)90083-2](https://doi.org/10.1016/0001-6160(53)90083-2).
- Pranke, Katja, Wendler, Marco, Weidner, Anja, Guk, Sergey, Weiß, Andreas, Kawalla, Rudolf, 2015. Formability of strong metastable Fe–15Cr–3Mn–3Ni–0.2C–0.1N austenitic TRIP/(TWIP) steel – a comparison of different base materials. *J. Alloys Compd.* 648, 783–793. <https://doi.org/10.1016/j.jallcom.2015.06.205>.
- Talonen, J., Aspegren, P., Hänninen, H., 2004. Comparison of different methods for measuring strain induced  $\alpha$ -martensite content in austenitic steels. *Mater. Sci. Technol.* 20 (12), 1506–1512. <https://doi.org/10.1179/026708304X4367>.
- Tamura, I., 1982. Deformation-induced martensitic transformation and transformation-induced plasticity in steels. *Met. Sci.* 16 (5), 245–253. <https://doi.org/10.1179/030634582790427316>.
- Totten, George E., 2006. *Steel Heat Treatment*. CRC Press.
- Weiß, Andreas, Gutte, Heiner, Mola, Javad, 2016. Contributions of  $\epsilon$  and  $\alpha'$  TRIP effects to the strength and ductility of AISI 304 (X5CrNi18-10) austenitic stainless steel. In *MTA* 47 (1), 112–122. <https://doi.org/10.1007/s11661-014-2726-y>.